

Seeing Radio: From Zero RF Priors to Explainable Modulation Recognition with Vision Language Models

Hang Zou*, Bohao Wang*[†], Yu Tian*, Lina Bariah*, Chongwen Huang[†], Samson Lasaulce[‡], Mérouane Debbah*

* 6G Research Center, Khalifa University, 127788 Abu Dhabi, UAE

[†] College of Information Science and Electronic Engineering, Zhejiang University, 310027, Hangzhou, China

[‡]Université de Lorraine, CNRS, CRAN, F-54000 Nancy, France

Abstract—The rise of vision language models (VLMs) paves a new path for radio frequency (RF) perception. Rather than designing task-specific neural receivers, we ask if VLMs can learn to recognize modulations when RF waveforms are expressed as images. In this work, we find that they can. In specific, in this paper, we introduce a practical pipeline for converting complex IQ streams into visually interpretable inputs, hence, enabling general-purpose VLMs to classify modulation schemes without changing their underlying design. Building on this, we construct an RF visual question answering (VQA) benchmark framework that covers 57 classes across major families of analog/digital modulations with three complementary image modes, namely, (i) short time-series IQ segments represented as real/imaginary traces, (ii) magnitude-only spectrograms, and (iii) joint representations that pair spectrograms with a synchronized time-series waveforms. We design uniform zero-shot and few-shot prompts for both class-level and family-level evaluations. Our finetuned VLMs with these images achieve competitive accuracy of 90% compared to 10% of the base models. Furthermore, the fine-tuned VLMs show robust performance under noise and demonstrate high generalization performance to unseen modulation types, without relying on RF-domain priors or specialized architectures. The obtained results show that combining RF-to-image conversion with promptable VLMs provides a scalable and practical foundation for RF-aware AI systems in future 6G networks.

Index Terms—Vision language models, radio frequency signals, modulation classifications, spectrograms

I. INTRODUCTION

Large language models (LLMs) have evolved rapidly in both scale and capability, becoming increasingly versatile across diverse applications. Through scaling laws and instruction tuning, they have enabled outstanding general-purpose reasoning and strong few-shot learning performance across a wide range of tasks [1]. Building on this progress, multimodal LLMs have emerged, bridging vision and language by pairing frozen or jointly trained vision encoders with powerful LLM backbones to ground linguistic reasoning in visual context [2]–[4]. As this evolution accelerates, foundation models such as GPT-5 demonstrate robust multimodal comprehension and strong cross-domain generalization, integrating textual and visual knowledge to solve more complex reasoning tasks [5].

In a parallel race, the 6G research agenda anticipates AI-native networks that can orchestrate sensing, communications, computing, and control at unprecedented scales and latencies. Accordingly, existing surveys and position papers emphasize

on the foundational integration of advanced AI technologies throughout the entire network stack, from radio access to core network automation, network slicing, and semantic communication [6]–[8]. Within this vision, LLMs emerge as unified interfaces for knowledge access, tool-use, reasoning and planning, supporting automated policy optimization, intelligent fault diagnosis, and intent-driven network operations for complex, heterogeneous infrastructures.

Early researches on *LLM4Telecom* have explored LLM-driven network and service management assistants, domain-specialized instruction-tuned models, and agentic workflows that integrate LLMs into network tools and monitoring data [9]–[13]. These studies have showcased promising results in network troubleshooting, configuration generation, root cause analysis, and closed-loop operations. However, they mainly rely on language, in the form of text, tables or structured logs, as the primary modality. Within this direction, Telecom-specific LLMs have been developed, such as TelecomGPT [14], to improve LLMs capabilities in telecom related tasks. Instead of relying on general-purpose LLMs or prompt engineering, telecom knowledge has been directly embedded into the LLMs to equip them with the needed operational intelligence, domain-grounded reasoning, and contextual understanding that are essential to reason over network scenarios and automate management tasks.

However, despite all this progress in Telecom LLMs, currently their integration into telecom networks is largely text-centric. Hence, this prevents the exploitation of such powerful tools in more advanced network tasks that require that an LLM can process and generate different kind of data modalities, including radio frequency (RF) signals, images, spectrograms, or acoustic signals, among others. It is worthy to note that future networks will not be only conversation- and reasoning-dependent, but they will also enjoy advanced RF perception capabilities.

Having said that, no existing vision language model (VLM) has been explicitly designed with spectrum intelligence, i.e., with capabilities to interpret or classify RF signal patterns. In telecom networks, such ability underpins a wide range of critical functions, including automatic modulation classification (AMC), interference detection, spectrum sensing, and signal quality analysis. These tasks are essential for dynamic

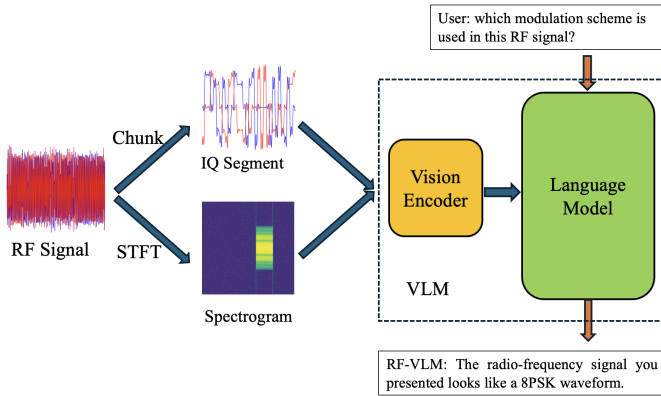


Fig. 1: Proposed framework. Spectrograms are obtained through STFT while IQ segment are obtained by down conversion and chunking. The VLM will be provided with image illustrating magnitude of spectrogram, IQ segment, or both of them.

spectrum access, cognitive radio, and autonomous network optimization, where understanding the underlying signal patterns enables adaptive communication.

Traditional AMC models rely on domain-specific deep networks, which are trained on IQ samples or spectrograms [15], but they often fail to generalize to unseen modulations and lack interpretability. On the other hand, VLMs have so far shown exceptional generalizability and multimodal-based reasoning capabilities, e.g., in audio spectrogram recognition [16]. Hence, the aim of our work is to explore the if RF understanding and perception can be directly linked to VLMs without redesigning model architectures or training them from scratch.

This paper proposes a simple, practical pipeline to enable off-the-shelf VLMs to understand raw RF IQ data, by converting them into visual representations that are interpretable by existing VLMs. Specifically, we transform RF signals into spectrograms using short-time Fourier transform (STFT) and into and as chunked IQ time-series panels, in order to construct a visual-question-answering (VQA) dataset, comprising queries on fine-grained modulation classes or higher-level signal categories. With lightweight fine-tuning and no architectural changes, we show that a modern VLM fine-tuned only on these images can perform *accurate modulation recognition while providing natural language explanations of their decisions*. Our main contributions are summarized as follows:

- We construct an efficient RF modulation classification benchmark covering spectrogram, time-series, and joint signal representations.
- We demonstrate, to the best of the authors' knowledge for the first time, that a general-purpose VLM can be adapted to classify RF modulations while producing concise, human-readable explanations.
- We show that, after minimal fine-tuning, the model achieves strong data efficiency and robustness to noise

and out-of-vocabulary (OOV) modulation classes, paving the way for RF-aware multimodal LLMs for 6G.

II. BENCHMARK DESIGN FOR RF MODULATION CLASSIFICATION

To assess the capability of VLMs in RF signal understanding, we construct a reproducible benchmark that evaluates VLMs on recognition of digital and analog modulation types from rendered RF visualizations. We leverage *TorchSig* [17] which provides 57 different modulation schemes across different families as follows:

- **OFDM (12):** Orthogonal Frequency-Division Multiplexing with different number of subcarriers $M \in \{64, 72, 128, 180, 256, 300, 512, 600, 900, 1024\}$ and $\{1200, 2048\}$.
- **QAM (8):** Quadrature Amplitude Modulation with constellation size $M \in \{16, 32, 64, 256, 1024\}$ plus cross-constellations: $\{32_cross, 128_cross, 512_cross\}$.
- **PSK (6):** Phase Shift Keying with different number of phase states $M \in \{2 (BPSK), 4 (QPSK), 8, 16, 32, 64\}$.
- **ASK (5):** Amplitude Shift Keying with different number of amplitude levels $M \in \{4, 8, 16, 32, 64\}$.
- **FSK (4):** Frequency Shift Keying with different number of distinct tones $M \in \{2, 4, 8, 16\}$.
- **GFSK (4):** Gaussian-filtered FSK with different number of distinct tones $M \in \{2, 4, 8, 16\}$.
- **MSK (4):** Minimum Shift Keying, constant-envelope CPM with different symbol alphabet size $M \in \{2, 4, 8, 16\}$.
- **GMSK (4):** Gaussian-filtered MSK with different symbol alphabet size $M \in \{2, 4, 8, 16\}$.
- **AM (4):** Amplitude Modulation (Analog) with different sideband type in Double-Sideband with carrier, Double-Sideband, Suppressed Carrier and Single-Sideband AM (Upper / Lower sideband only).
- **Chirp/LFM (3):** Linear Frequency Modulation with data-dependent chirp, Linear FM radar-style pulses and Chirp Spread Spectrum.
- **Singleton (3):** Frequency Modulation (FM), On-Off Keying (OOK) and un-modulated tone (Tone).

The benchmark supports three input image modes, namely, *IQ segment only (IQ)*, *spectrogram only (Spec)*, and *joint spectrogram and IQ (Joint)*, with deterministic pipelines for data synthesis, preprocessing and prompt design.

A. RF preprocessors and image input modes

IQ segment classification Given a complex baseband sequence of length N , $x[n] \in \mathbb{C}$, which can be obtained by down conversion of an RF signal, we visualize a short segment of the *in-phase* ($\Re\{x[n]\}$) and *quadrature* ($\Im\{x[n]\}$) components as two time series traces. Let $r[n] = \Re\{x[n]\}$ denotes the real component. To extract the underlying patterns from the RF waveform, we define zero-crossing points with a predefined hysteresis ϵ :

$$ZC = \{n \mid r[n-1] \leq \epsilon, r[n] > \epsilon\}. \quad (1)$$

These zero-crossing points capture local oscillatory behavior and phase transitions, providing patterns that can be visually represented and classified by a VLM.

Given integers N_{\min} and N_{\max} , we sample an integer $P \sim \mathcal{U}\{N_{\min}, N_{\max}\}$ and extract the shortest contiguous segment that contains P zero-crossing intervals. We avoid a fixed sample length because different carrier/symbol rates yield different oscillation rates, hence, a fixed window will show a variable number of cycles and distort the waveform's visual geometry across modulation classes. By counting periods instead, we normalize the time axis and ensure that each segment contains a consistent number of signal cycles, regardless of symbol rate or sampling configuration. Note that this preprocessing only selects the segment, i.e., the VLM still receives the raw IQ traces for that window (no additional temporal filtering or phase decoding).

Spectrogram classification We compute an STFT with window $w[n]$, fast Fourier transform (FFT) size K , and hop H ,

$$S[k, t] = \sum_n x[n] w[n - tH] e^{-j2\pi kn/K}, \quad k \in [0, K-1] \quad (2)$$

A Blackman window is used, with no centering and an FFT shift applied along the frequency axis. We render a magnitude spectrogram $|S[k, t]|$ in dB, followed by robust per-image normalization and a perceptually uniform colormap (e.g., `viridis`), ensuring that amplitude variations are visually consistent and comparable across modulation types. This time-frequency representation gives unique spectral patterns, such as symbol transitions, bandwidth occupancy, and sideband structures, allowing the VLM to differentiate between modulation schemes through visual hints rather than explicit signal models.

Joint spectrogram and IQ segment classification We simply concatenate the spectrogram with an IQ segment along the width. Each image consists of two horizontal panels, namely magnitude spectrogram on left and IQ time-series on right (real in blue, imag in red). The panels are height-matched before concatenation.

The resolutions of all images are aligned with the FFT size to avoid compression error introduced during resizing. For both spectrograms and IQ segments no time or frequency axis are provided so that the VLM will focus on the pattern itself and avoid leaking from legend for all image modes. The proposed method is summarized in Fig. 1.

B. Prompt Design

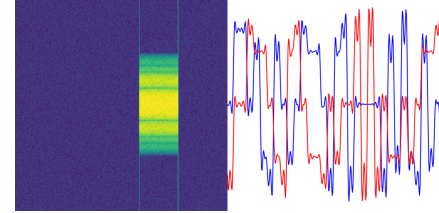
We support both *zero-shot* (with no examples provided) and *few-shot* (with few examples provided) evaluations with n -way (selecting the correct one among n choices) classification:

- **Zero-shot n -way:** Each record contains (i) a *query* image, (ii) a list of n candidate classes, uniformly sampled without replacement (balanced target cycling), and (iii) the gold label.
- **Few-shot n -way, s -shots:** For each candidate class we attach s example images (disjoint from the query) before

VQA Prompt Template for Modulation Classification

System: You are a helpful assistant with expertise in recognizing patterns and identifying RF modulations from visual inputs.

User: Your task is to analyze an RF visualization and determine the most likely modulation class from a given list. Note: this image has two horizontal panels. LEFT: magnitude spectrogram (dB), RIGHT: a short IQ time-series panel showing *real* part (blue) and *imaginary* part (red) of the signal plotted over time. The time-series corresponds to a segment down converted from the RF waveform. Here are the classes: ['am-dsb', 'ofdm-128', '16gmsk', '4fsk', 'ook', '16ask', '16psk', '8ask', '32ask', 'ofdm-300']. Your response must contain the exact name of the class only. Here is the **IMAGE**:



VLM: {modulation-class}

Fig. 2: VQA-style prompt template for zero-shot RF modulation 10-way classification provided a concatenation of spectrogram magnitude and the IQ time series segment.

the query image. Examples and queries are drawn from different splits to avoid data leakage.

We use a simple chat-style schema with `system` and `user` roles to construct inputs for VLMs:

Zero-shot prompts The `system` prompt states that the model will see RF signals (spectrograms and/or IQ panels) and must classify from a given list. The `user` message contains:

- 1) A concise instruction: “*Your task is to analyze an RF visualization and determine the most likely modulation class in the following list: [C₁, ..., C_n].*”
- 2) A *mode-specific note*, automatically attached based on the image mode:
 - **Spec:** includes only the spectrogram magnitude (in dB), without phase information or no time-domain waveform.
 - **IQ:** includes a short IQ time-series panel showing real part (blue) and imaginary part (red) of the signal plotted over time, without spectrogram views.
 - **Joint:** includes a combination of both representations; encouraging the model to combine spectral and temporal patterns.

Few-shot prompts: To help the model ground its reasoning, we begin with a short introductory instruction: “*You will see*

Model	Image Mode	Zero-shot	1-shot	2-shot
InternVL3-8B	Spec	9.70%	20.75%	24.67%
	IQ	10.70%	23.68%	26.84%
	Joint	9.80%	21.45%	26.95%
Qwen2.5-VL-7B-Instruct	Spec	12.68%	24.76%	30.71%
	IQ	15.40%	32.33%	36.25%
	Joint	11.50%	27.65%	29.45%
GPT5-Nano	Spec	18.2%	30.0%	27.8%
	IQ	17.1%	18.1%	21.2%
	Joint	16.0%	31.4%	22.2 %

TABLE I: Overall accuracy (%) of VLMs on RF modulation classification across different shots and image modes.

examples for several classes, followed by a query image. Use frequency patterns (spectrogram) and temporal dynamics (IQ waveforms) as appropriate.” Then, for each candidate class c_i , we add s example images labeled “Spectrogram (and/or time-series panels) for c_i ”. Finally, we add the query block with the same instruction as zero-shot and the query image(s). VLMs are always required to return only the exact class name.

III. VLMs ARE RF SIGNAL CLASSIFIERS AFTER FINE-TUNING

A. General-purpose VLMs Fail to Generalize to RF Domains

We start with benchmarks built with *noiseless* RF signals. We set FFT size $K = 512$ with hop $H = 256$, with each time series waveform contains 20-25 zero-crossing intervals. We evaluate popular commercial and open-sourced VLMs on our benchmark over 10-way 1000 VQAs for each image mode. For commercial VLMs, we consider GPT5-nano [5] while Qwen2.5-VL-7B-Instruct [3] and InternVL3-8B [4] are selected among open-sourced ones. We report the zero-shot and few-shots evaluations of the above models in Table I. We first observe that considered VLMs possess almost no prior knowledge of the spectral or temporal representations of RF signals and struggle to learn such domain-specific patterns through few-shot in-context learning. These results indicate that pretrained VLMs lack usable priors for RF time-frequency patterns and do not acquire them via in-context prompting alone. Next, we examine whether lightweight, parameter-efficient fine-tuning (PEFT) can close this gap.

B. Parameter-Efficient Fine-Tuning Enables RF Signal Recognition

To quantify domain adaptation ability of VLMs, we apply PEFT to VLMs using QLoRA [18], which has proven effective for adapting LLMs to specialized domains. We fine-tune two open-sourced VLMs using a workstation equipped with two Nvidia A6000 GPUs. The LoRA rank and scaling factor are fixed at $r = 32$ and $\alpha = 64$, respectively. Each model is trained for 5 epochs with a learning rate of 2×10^{-4} on a dataset containing all image modes and 57 modulation classes, totaling 20K samples, approximately 350 samples per class. We denote the fine-tuned VLMs with the suffix “-RF”.

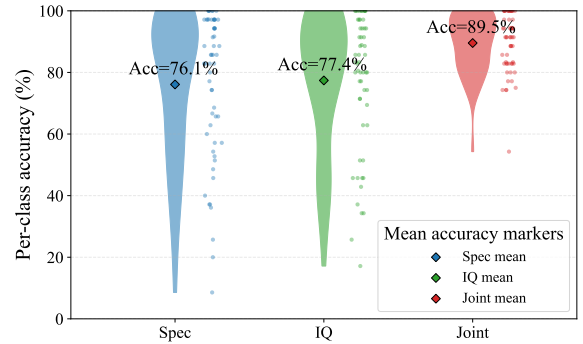


Fig. 3: Per-class accuracy distribution of Qwen2.5-VL-7B-Instruct-RF.

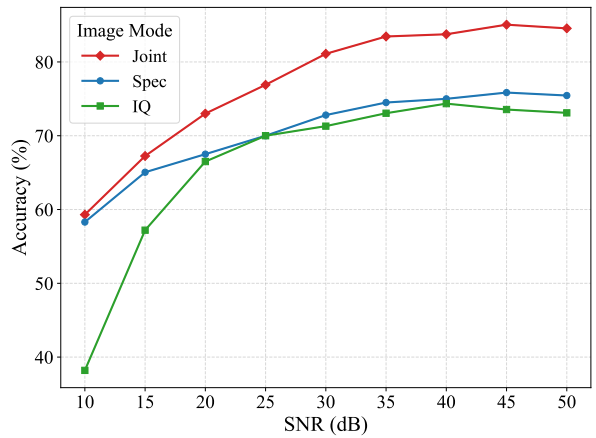


Fig. 4: Accuracy vs. SNR of Qwen2.5-VL-7B-Instruct-RF under different image modes.

As shown in Table II and Fig. 3, fine-tuning leads to substantial accuracy gains across all visual representations from around 10% to around 80%. For Qwen2.5-VL-7B-Instruct-RF, the joint representation achieves 89.55% accuracy, outperforming both the spectrogram-only (76.1%) and IQ-only representations (77.40%). Similarly, InternVL3-8B-RF reaches the highest 91.20% with joint representation. Across all modulation families and visual representations, the joint representation consistently outperforms individual modalities. In particular, it significantly boosts weaker IQ-only families, such as OFDM (from 44.36% to 89.78%), and AM (from 65.0% to 92.14%), while maintaining strong performance on spectrally distinctive families, including FSK, GFSK, and Chirp/LFM. These results demonstrate that fusing spectral and temporal information allows VLMs to jointly capture frequency-domain stability and time-domain dynamics, leading to more discriminative and generalizable modulation features. The joint representation therefore provides a strong basis for extending the proposed framework toward modality-robust and domain-adaptive understanding of RF signals for VLMs.

Model	Image Mode	w/o FT	With FT	ASK	FSK	GFSK	GMSK	MSK	QAM	PSK	OFDM	AM	Chirp/LFM	OOK	Tone
Qwen2.5-VL-7B-Instruct	Spec	12.68%	76.10%	65.14%	98.57%	93.57%	87.86%	94.29%	47.43%	33.64%	84.54%	88.57%	92.16%	97.14%	100.00%
	IQ	15.40%	77.40%	77.14%	95.72%	90.71%	92.86%	97.86%	79.06%	90.53%	44.36%	65.00%	87.26%	100.00%	100.00%
	Joint	11.50%	89.55%	76.57%	100.00%	94.29%	92.14%	94.29%	78.72%	91.98%	89.78%	92.14%	95.75%	100.00%	100.00%
InternVL3-8B	Spec	9.70%	77.35%	66.29%	98.57%	94.29%	91.43%	100.00%	45.61%	35.61%	86.45%	88.57%	92.88%	100.00%	100.00%
	IQ	10.70%	77.60%	78.86%	94.29%	89.29%	88.57%	98.57%	82.97%	86.37%	45.12%	72.86%	83.69%	97.14%	100.00%
	Joint	9.80%	91.20%	82.28%	97.86%	94.29%	90.71%	99.29%	85.06%	93.45%	90.24%	92.14%	95.04%	100.00%	100.00%

TABLE II: Average accuracy (%) with and without finetuning (FT) and per-family accuracies (%) of VLMs.

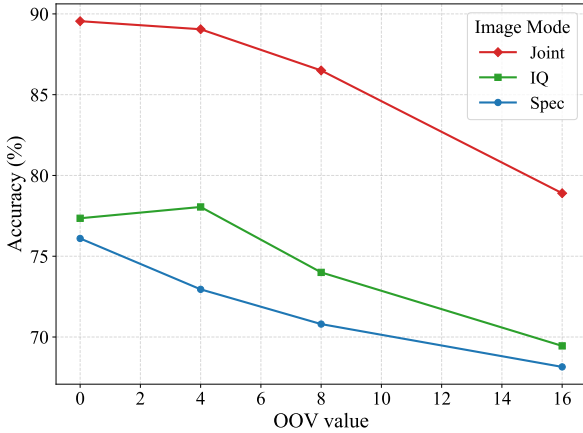


Fig. 5: Accuracy vs. number of OOV classes of Qwen2.5-VL-7B-Instruct-RF under different image modes.

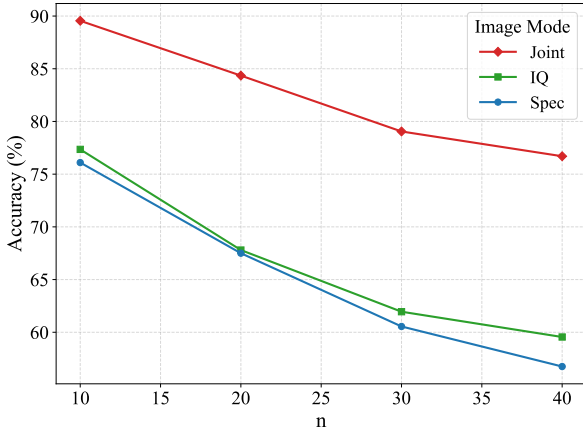


Fig. 6: Accuracy vs. number of choices of Qwen2.5-VL-7B-Instruct-RF under different image modes.

C. Noise Robustness Evaluation

To evaluate the noise robustness of our visual representations, we fine-tuned Qwen2.5-VL-7B-Instruct on a mixed dataset covering signal-to-noise (SNR) values from 10 dB to 50 dB. Each VLM was separately tested at discrete SNR levels varying from 10 dB to 50 dB with a step size of 5 dB, as illustrated in Fig. 4.

Across all image modes, we noticed a steady improvement of accuracy with higher SNR levels, confirming that each

representation benefits from improved signal quality. Notably, the joint representation experiences a faster increase rate than the spectrogram-only and IQ-only modes, improving from approximately 59.3% at 10 dB to about 83.45% at 35 dB, after which performance plateaus. This trend reflects the fact that the IQ-only representation, which is highly sensitive to temporal fluctuations, becomes ineffective under heavy noise (e.g., at 10 dB) and thus cannot exploit the full signal structure. By contrast, the joint representation combines both spectral stability and temporal dynamics and is therefore better able to leverage the improved conditions at higher SNR values. These results demonstrate that the joint representation consistently delivers superior noise robustness.

D. Out-of-Vocabulary Modulation Evaluation

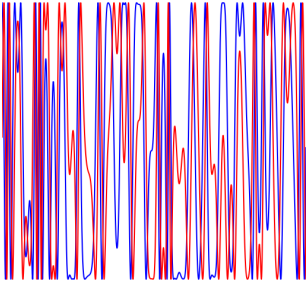
To further assess generalization under open-set conditions, we ran additional OOV experiments. We randomly excluded 4, 8, and 16 modulation classes from the full set of 57 during training while retaining the full label space at evaluation. This setup tests whether models rely on learned visual–semantic associations rather than closed-set memorization. As shown in Fig. 5, accuracy decreases for all image modes as the number of unseen classes grows. The joint representation maintains the highest absolute accuracy at every OOV level (e.g., from 89.55% with no OOV classes to 78.90% with 16 OOV classes, a drop of 11 percentage points), whereas spectrogram-only is somewhat less sensitive (from 76.10% to 68.15%, a drop of 8 points) but remains lower in absolute performance. The IQ-only mode exhibits intermediate sensitivity and overtakes spectrogram-only as more classes are withheld. Joint time–frequency cues yield the strongest OOV recognition overall, but mitigating their slightly higher sensitivity to open-set shift is a promising direction for future work.

E. Impact of Number of Classes in VQA

We primarily evaluate 10-way classification, but also examine how accuracy scales as the number of distractor classes increases. In Fig. 6, we illustrate the classification accuracy versus the number of candidate classes for Qwen2.5-VL-7B-Instruct-RF. As expected, the accuracy of all representations decreases as the number of classes increases. As observed in other evaluations, joint representation outperforms the others largely with a gain of around 15% in average while the performance of IQ-only representation slightly dominates the spectrogram-only one. The decline is largely driven by hard negatives from the same modulation family that differ only by

RF Modulation Classification with Explanation

User: Select the correct modulation class in [‘qpsk’, ‘8gmsk’, ‘ook’, ‘fm’, ‘512qam-cross’, ‘4msk’, ‘4fsk’, ‘ofdm-180’, ‘8msk’, ‘16psk’] for following RF signal with your rationale:



VLM: The waveform exhibits significant power onset latency and bandwidth expansion starting at the first significant power onset. This suggests a modulation scheme with complex temporal patterns beyond simple harmonics. The presence of harmonics spaced at intervals corresponding to the fundamental frequency indicates a bandwidth-rich signal class. Considering the harmonics and temporal structure, the most likely class from the given list is ‘fm’.

Fig. 7: RF modulation classification with explanation.

parameters (e.g., OFDM subcarrier count, QAM constellation size), for which the generic visual encoder produces highly similar features. This suggests current image encoder in VLMs lack the fine-grained discriminative cues needed to separate near-neighbor classes. A promising direction is to pretrain an RF-aware visual encoder on temporal or spectral views, strengthening fine-grained discrimination as the number of distractors grows.

F. Modulation Classification with Explanations

Having established that fine-tuned VLMs can accurately classify RF modulations across different image modes, we next investigate how these models reason about their decisions. To achieve this, we prompt the models to generate textual explanations with each prediction. As illustrated in Fig. 7, Qwen2.5-VL-7B-Instruct-RF correctly identifies FM from an IQ-segment input and provides a reasonable justification related to observing the signal structure. Notably, no explanation supervision was used during fine-tuning, yet the model often articulates domain-relevant insights. However, such rationales are not guaranteed to be reliable, as they may reflect language priors rather than evidence actually used by the vision pathway, risking hallucination. Incorporating grounding mechanisms, such as highlighting the visual evidence, testing counterfactual examples, or verifying through retrieval, offers a promising path to improve faithfulness and trustworthiness.

IV. CONCLUSION

In this work, we aimed to evaluate whether off-the-shelf VLMs can recognize RF modulations, when RF waveforms are converted into different visual representations. We demonstrated accordingly that, while vanilla VLMs show little prior ability and few-shot in-context learning remains ineffective, lightweight parameter-efficient fine-tuning within our RF-to-image pipeline enables them to perform competitive modulation classification without any architectural changes.

Pairing a spectrogram with a short IQ trace yields the best accuracy, strong noise robustness, non-trivial OOV generalization, and clear human-readable explanations, building a practical bridge between RF data and general-purpose VLMs. Future work will explore more realistic datasets and richer channel conditions, add grounding and calibration to explanations, and extend the approach to wideband, multi-label, and streaming RF scenarios.

REFERENCES

- [1] T. B. Brown *et al.*, “Language Models are Few-Shot Learners,” in *Advances in Neural Information Processing Systems (NeurIPS)*, 2020.
- [2] H. Liu *et al.*, “Visual instruction tuning,” *Advances in Neural Information Processing Systems*, vol. 36, pp. 34 892–34 916, 2023.
- [3] S. Bai *et al.*, “Qwen2.5-VL Technical Report,” *arXiv preprint arXiv:2502.13923*, 2025.
- [4] J. Zhu *et al.*, “InternVL3: Exploring Advanced Training and Test-Time Recipes for Open-Source Multimodal Models,” *arXiv preprint arXiv:2504.10479*, 2025.
- [5] OpenAI, “Introducing GPT-5,” *OpenAI Blog*, 2025.
- [6] A. Shahid *et al.*, “Large-scale AI in telecom: Charting the roadmap for innovation, scalability, and enhanced digital experiences,” *arXiv preprint arXiv:2503.04184*, 2025.
- [7] Y. Zhao *et al.*, “A Comprehensive Survey of 6G Wireless Communications,” *arXiv preprint arXiv:2101.03889*, 2020.
- [8] M. Giordani *et al.*, “6G: The Intelligent Network of Everything – A Comprehensive Vision and Tutorial,” *arXiv preprint arXiv:2407.09398*, 2024.
- [9] L. Liang *et al.*, “Large Language Models for Wireless Communications: From Adaptation to Autonomy,” *arXiv preprint arXiv:2507.21524*, 2025.
- [10] F. Zhu *et al.*, “Wireless large ai model: Shaping the ai-native future of 6g and beyond,” *arXiv preprint arXiv:2504.14653*, 2025.
- [11] J. Shao *et al.*, “WirelessLLM: Empowering Large Language Models Towards Wireless Intelligence,” *arXiv preprint arXiv:2405.17053*, 2024.
- [12] L. Bariah, Q. Zhao, H. Zou, Y. Tian, F. Bader, and M. Debbah, “Large Generative AI Models for Telecom: The Next Big Thing?” *IEEE Communications Magazine*, vol. 62, no. 11, pp. 84–90, 2024.
- [13] H. Zhou *et al.*, “Large Language Model (LLM) for Telecommunications: A Comprehensive Survey on Principles, Key Techniques, and Opportunities,” *IEEE Communications Surveys & Tutorials*, vol. 27, no. 3, pp. 1955–2005, 2025.
- [14] H. Zou, Q. Zhao, Y. Tian, L. Bariah, F. Bader, T. Lestable, and M. Debbah, “TelecomGPT: A Framework to Build Telecom-Specific Large Language Models,” *IEEE Transactions on Machine Learning in Communications and Networking*, vol. 3, pp. 948–975, 2025.
- [15] X. Liu, D. Yang, and A. El Gamal, “Deep Neural Network Architectures for Modulation Classification,” *arXiv preprint arXiv:1712.00443*, 2017.
- [16] S. Dixit *et al.*, “Vision language models are few-shot audio spectrogram classifiers,” in *Audio Imagination: NeurIPS 2024 Workshop AI-Driven Speech, Music, and Sound Generation*, 2024.
- [17] L. Boegner *et al.*, “Large scale radio frequency signal classification,” *arXiv preprint arXiv:2207.09918*, 2022.
- [18] T. Dettmers *et al.*, “QLoRA: Efficient Finetuning of Quantized LLMs,” in *Advances in Neural Information Processing Systems*, vol. 36, 2023, pp. 10 088–10 115.